

# Femtosecond optical frequency comb-based tandem interferometer

**Dong Wei**

[weidong@nanolab.t.u-tokyo.ac.jp](mailto:weidong@nanolab.t.u-tokyo.ac.jp)

**Satoru Takahashi**

[takahashi@nanolab.t.u-tokyo.ac.jp](mailto:takahashi@nanolab.t.u-tokyo.ac.jp)

**Kiyoshi Takamasu**

[takamasu@pe.t.u-tokyo.ac.jp](mailto:takamasu@pe.t.u-tokyo.ac.jp)

**Hirokazu Matsumoto**

[hi.matsumoto@nanolab.t.u-tokyo.ac.jp](mailto:hi.matsumoto@nanolab.t.u-tokyo.ac.jp)

Department of Precision Engineering, The University of Tokyo, Hongo 7-3-1, Bunkyo-ku, Tokyo 113-8656, Japan

Department of Precision Engineering, The University of Tokyo, Hongo 7-3-1, Bunkyo-ku, Tokyo 113-8656, Japan

Department of Precision Engineering, The University of Tokyo, Hongo 7-3-1, Bunkyo-ku, Tokyo 113-8656, Japan

Department of Precision Engineering, The University of Tokyo, Hongo 7-3-1, Bunkyo-ku, Tokyo 113-8656, Japan

The principle of a unique interferometer, called a femtosecond optical frequency comb-based (FOFC-based) tandem interferometer, is proposed and demonstrated for the first time. By taking advantage of both the temporal coherence characteristic of an FOFC light source and the transmission characteristics of acquired length information based on a tandem interferometer, the present technique is expected to be useful for high-precision measurement of long distances for not only science purposes but also industry requirements. [DOI: 10.2971/jeos.2009.09043]

**Keywords:** mode-locked lasers, frequency comb, tandem interferometer, ultrafast phenomena, temporal coherence

## 1 INTRODUCTION

Remote measurements of lengths are strongly demanded for not only science purposes but also industry requirements. Remote length measurement systems must have rapid response and high precision in space mission projects such as DARWIN and LISA [1]. Due to its increased frequency stability and very broad frequency band, the femtosecond optical frequency comb (FOFC) is a good choice for high-precision long-distance measurements [1]–[8]. With the internationalization of production supply, however, the necessity for accurate and economical remote calibration measurements continues to increase. For remote measurements, tandem low-coherence interferometers have been used, because the length information can be transmitted between two separated places [9]–[11]. We have investigated the temporal coherence function of a pulse train from an FOFC [12, 13]. The results show that high temporal coherence peaks exist during the period equal to the repetition intervals in the traveling direction of the FOFC.

Based on these previous works, in the present study, we demonstrate an FOFC-based tandem interferometer. As shown below, in the FOFC-based tandem interferometric scheme, a long optical-path difference is recorded by different pairs of pulse trains from the FOFC, transmitted by the unique character of a tandem interferometer, and then “compressed” and measured by the temporal interference between the different pairs of pulse trains. Fortunately, this new approach to high-accuracy length metrology, by combining the FOFC light source and a tandem interferometer, has its own advantages. The FOFC-based tandem interferometer enables long optical-path difference measurement by nonsymmetrical

tandem configurations in a relatively small well-calibrated reference system. For simplicity of explanation, we have neglected the dispersion and absorption of the optical devices over the FOFC’s illumination bandwidth. We note that in 2009, a numerical model of pulse train propagation in air was reported and was applied to length measurements by using interference fringes between chirped pulses [7, 8].

## 2 PRINCIPLE

Figure 1 shows an overview of the developed system. The optical scheme is carried out with a system consisting of an FOFC optical source, a tandem interferometer, and system controls. The FOFC optical source’s power spectrum can be expressed as follows,

$$P(f) \propto A(f - f_c) \times \text{comb}(f_{\text{rep}}),$$

$$\text{comb}(f_{\text{rep}}) \equiv \sum_{m=-\infty}^{+\infty} \delta(f - mf_{\text{rep}}) \quad (1)$$

where  $A(f - f_c)$  is the envelope function of the FOFC power spectrum and  $f_c$  is the center carrier frequency of the FOFC. When the electric field packet repeats at the pulse repetition period  $T_R$ , the “carrier” phase slips by  $\Delta\phi_{ce}$  to the carrier-envelope phase because of the difference between the group and phase velocities. In the frequency domain, a mode-locked FOFC generates equidistant frequency comb lines with the pulse repetition frequency  $f_{\text{rep}} \propto 1/T_R$ . Based on the Wiener-Khintchine theorem, the interferometric signal of the autocor-

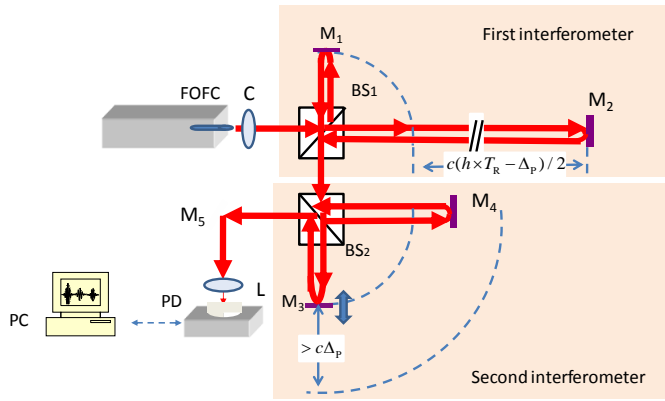


FIG. 1 System overview of the FOFC-based tandem interferometer FOFC: femtosecond optical frequency comb, BS<sub>1-2</sub>: beam splitters, M<sub>1-5</sub>: mirrors, C: collimator, L: lens, PD: photo detector, PC: personal computer.

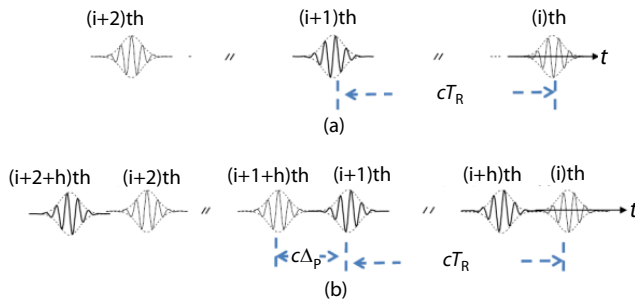


FIG. 2 Relative delay between pulse trains formed by an unbalanced optical-path Michelson interferometer (first interferometer). (a) Relative positions of the pulse train before introduction into the first interferometer. (b) Relative positions of two pulse trains after traveling by the first interferometer.

relation function is given by

$$\gamma(\tau) \propto \mathcal{F}^{-1} [A(f - f_c)] \otimes \text{comb}(T_R),$$

$$\text{comb}(T_R) \equiv \sum_{m=-\infty}^{+\infty} \delta(\tau - mT_R). \quad (2)$$

From Eq. (2), the temporal coherence function periodically displays a high temporal coherence peak where the pulse trains signal of the FOFC displays a high-intensity peak with the pulse repetition period  $T_R$ .

The optical scheme of a tandem interferometer is shown in Figure 1. The tandem interferometer has a tandem configuration of two unbalanced optical-path Michelson interferometers. The first interferometer is composed of a beam splitter (BS<sub>1</sub>), a fixed reference mirror (M<sub>1</sub>), and an object mirror (M<sub>2</sub>). The pulse train from an FOFC light source is introduced into the first interferometer and split into two identical parts at the BS<sub>1</sub>, and then  $E_{\text{train1}}(t)$  is reflected by M<sub>1</sub> and  $E_{\text{train2}}(t)$  is reflected by M<sub>2</sub>.  $E_{\text{train2}}(t)$  is delayed relative to  $E_{\text{train1}}(t)$  with  $l = c(h \times T_R - \Delta_P)/2$  ( $c$  is the light velocity in air,  $h = \text{floor}(2l/cT_R)$ ,  $\Delta_P = \text{mod}(2l, cT_R)$ ), and they are finally recombined at the BS<sub>1</sub> (see Figure 2).

After travelling by the first interferometer, the recombined pulse trains are introduced into the second interferometer. The second interferometer of the tandem interferometer is com-

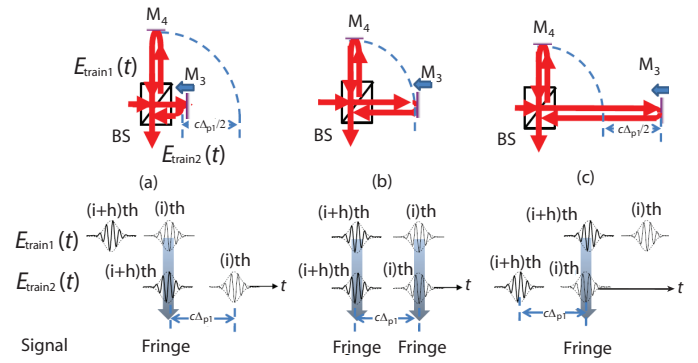


FIG. 3 Interference fringes form with different relative delays between pulse trains formed by the second interferometer. With relative optical-path delay as (a)  $-c\Delta_{P1}$ , (b) 0 and (c)  $c\Delta_{P1}$ . The relatively delayed pulse trains will overlap as (d), (e) and (f) respectively and the expected interference fringes can be observed.

posed of a BS<sub>2</sub>, a moving reference mirror (M<sub>3</sub>), which is fixed on the top surface of a computer-controlled and calibrated ultrasonic stepping motor, and a fixed object mirror (M<sub>4</sub>). The recombined pulse trains from BS<sub>1</sub> are split into two identical parts at the BS<sub>2</sub>, and then  $E_{\text{train3}}(t)$  is reflected by M<sub>3</sub> and  $E_{\text{train4}}(t)$  is reflected by M<sub>4</sub>.  $E_{\text{train3}}(t)$  is delayed relative to  $E_{\text{train4}}(t)$  with different relative optical-path delays, as shown in Figure 3, and they are finally recombined at the BS<sub>2</sub>. When relative optical-path delay is 0, the interference fringes (auto correlation patterns) can be observed as an ordinary Michelson interferometer. The optical comb mode-lock technique results in interference fringes (cross correlation patterns) reappearing at delays equal to  $-c\Delta_{P1}$  and  $c\Delta_{P1}$  between different pairs of pulse trains. When the pulse trains  $E_{\text{train4}}(t)$  and the relatively delayed pulse trains  $E_{\text{train3}}(t)$  finally overlap at the BS<sub>2</sub> (see Figures 3(d) and 3(f)), one can expect that interference fringes will be observable. After performing the time integration, we obtain

$$I(t) \propto |\gamma(\tau)| \cos [\text{mod}(h \times \Delta\phi_{ce}, 2\pi)]. \quad (3)$$

### 3 EXPERIMENT

The experiment is carried out with an FOFC (FC1500, MenloSystems,  $f_{\text{rep}} = 100$  MHz). The pulse trains from the FOFC are expanded and collimated by a collimator (C<sub>1</sub>) and introduced into the tandem interferometer. In the first interferometer, the relative optical displacement  $c(h \times T_R - \Delta_P)/2$  between the two pairs of pulse trains is about 1.5 m ( $h = 1$ ). During the measurement, by moving M<sub>3</sub> by means of a computer-controlled and calibrated ultrasonic stepping motor, we could observe the interference fringes. After travelling different path lengths, these two pairs of pulse trains overlap at the BS<sub>2</sub>. Lens L makes an image of the interference fringes on a photo detector (PD).

Figure 4 illustrates the acquired interference fringes. The three interference fringe signals exhibit a high contrast between the two pairs of pulse trains by the relative optical displacements  $-c\Delta_P$ , 0 and  $c\Delta_P$  respectively. To distinguish the real interference fringe peaks from the side lobes of the second interference fringes, we move M<sub>2</sub>, which means the first and third

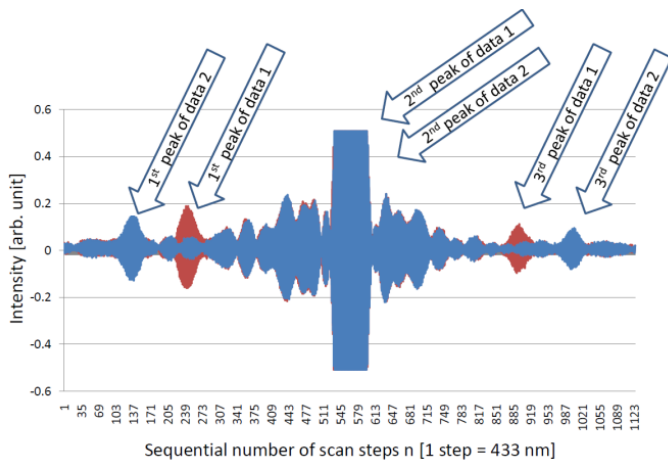


FIG. 4 Interference fringes with different relative delays between two pulse trains.

interference fringes will exhibit high contrasts with a different relative optical displacement,  $-c\Delta p$  and  $c\Delta p$ . As noted in Figure 4, the first and third peaks move away from the second interference fringes peak (the two peaks of the second interference fringes overlap).

Figure 5 shows the result when a  $50\ \mu\text{m}$  step displacement by the shift of  $M_2$  was repeatedly induced over a distance range of  $500\ \mu\text{m}$ . We fitted the centers of the peaks, and measured the relative displacement between the two peaks. The obtained experimental value of the change in relative displacement is  $50 \pm 2.45\ \mu\text{m}$ . And as shown in Figure 5, we obtained the good linearity between the change in the step displacement shift of  $M_2$  and the measured change in relative displacement between two peaks. The measured result of distance is in good agreement with the set distance value by shift of  $M_2$  within a standard deviation.

During the measurements, the fluctuations of displacement between two peaks due to noise, such as mechanical vibration and temperature fluctuation, in the state were monitored. The effect of the shift of  $M_2$  with  $50\ \mu\text{m}$  step displacement is sufficiently larger than that due to noise.

The measuring range is mainly affected by the range of the stepping motor. The experimental resolution suffers primarily

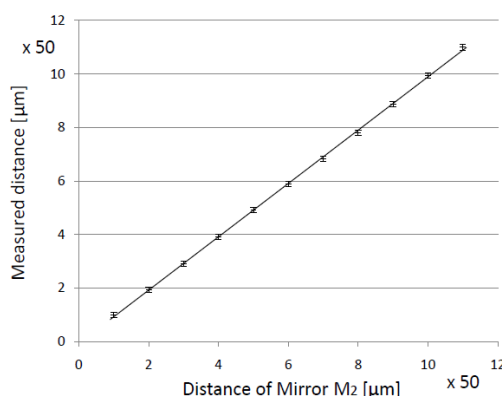


FIG. 5 Measurement result by a step displacement shift of  $M_2$  and measured displacement.

from the error arising from peak overlap caused by the side lobe noise on interference fringes due to the restricted resolution of the oscilloscope. However, it should be stressed that these limitations are not related to the principle itself. We are currently pursuing an approach in which performance can be improved using an optical device with high accuracy and an appropriate design of the system.

## 4 SUMMARY

In summary, we proposed the concept and the principle of an FOFC-based tandem interferometry technique. The unique feature of an FOFC-based tandem interferometer is that high temporal coherence peaks can be observed between different pairs of phase pulses from the FOFC light source, and the length information can be transmitted and “compressed” between two separated places such as a calibration laboratory and an individual satellite. The proof-of-the-principle experiments were presented and validated the proposed principle. This is, to the best of our knowledge, the first report on the principle and the experimental development of an FOFC-based tandem interferometer. The present technique is expected to be useful for the measurement of high-precision long distances for not only science purposes but also industry requirements.

## ACKNOWLEDGEMENTS

Part of this research work was supported by the Global Center of Excellence (COE) Program on “Global Center of Excellence for Mechanical Systems Innovation” granted to The University of Tokyo from the Japanese Government. We are also grateful to NEOARK Corporation for providing the femtosecond fiber laser. Dong Wei gratefully acknowledges the scholarship assistance provided by the Takayama International Education Foundation, Heiwa Nakajima Foundation, Ministry of Education, Culture, Sports, Science, and Technology of Japan, respectively.

## References

- [1] I. Coddington, W. C. Swann, L. Nenadovic, and N. R. Newbury, “Rapid and precise absolute distance measurements at long range” *Nat. Photonics* **3**, 351 (2009).
- [2] K. Minoshima, and H. Matsumoto, “High-accuracy measurement of 240-m distance in an optical tunnel by use of a compact femtosecond laser” *Appl. Opt.* **39**, 5512 (2000).
- [3] T. Yasui, K. Minoshima, and H. Matsumoto, “Stabilization of femtosecond mode-locked Ti:sapphire laser for high-accuracy pulse interferometry” *IEEE J. Quantum Elect.* **37**, 12 (2001).
- [4] Y. Yamaoka, K. Minoshima, and H. Matsumoto, “Direct measurement of the group refractive index of air with interferometry between adjacent femtosecond pulses” *Appl. Opt.* **41**, 4318 (2002).
- [5] J. Ye, “Absolute measurement of a long, arbitrary distance to less than an optical fringe” *Opt. Lett.* **29**, 1153 (2004).
- [6] M. Cui, R. N. Schouten, N. Bhattacharya, and S. A. Berg, “Experimental demonstration of distance measurement with a femtosecond frequency comb laser” *J. Eur. Opt. Soc.-Rapid* **3**, 08003 (2008).

- [7] M. Cui, M. G. Zeitouny, N. Bhattacharya, S. A. van den Berg, H. P. Urbach, and J. J. M. Braat, "High-accuracy long-distance measurements in air with a frequency comb laser" *Opt. Lett.* **34**, 1982 (2009).
- [8] P. Balling, P. K  en, P. Mařika, and S. A. van den Berg, "Femtosecond frequency comb based distance measurement in air" *Opt. Express* **17**, 9300 (2009).
- [9] A. Hirai, and H. Matsumoto, "Low-coherence tandem interferometer for measurement of group refractive index without knowledge of the thickness of the test sample" *Opt. Lett.* **28**, 2112 (2003).
- [10] H. Matsumoto, K. Sasaki, and A. Hirai, "103-km-long remote measurements of end standards using low-coherence optical-fiber tandem interferometer in experimental room" *Jpn. J. Appl. Phys.* **44**, 6287 (2005).
- [11] H. Matsumoto, and K. Sasaki, "Remote measurements of practical length standards using optical fiber networks and low-coherence interferometers" *Jpn. J. Appl. Phys.* **47**, 8590 (2008).
- [12] D. Wei, S. Takahashi, K. Takamasu, and H. Matsumoto, "Analysis of the temporal coherence function of a femtosecond optical frequency comb" *Opt. Express* **17**, 7011 (2009).
- [13] D. Wei, S. Takahashi, K. Takamasu, and H. Matsumoto, "Simultaneous observation of high temporal coherence between two pairs of pulse trains using a femtosecond-optical-frequency-comb-based interferometer" *Jpn. J. Appl. Phys.* **48**, 070211 (2009).